Interface of n-type WSe_2 photoanodes in aqueous solution. II. Photoelectrochemical properties

R. Bourezg, G. Couturier, and J. Salardenne
Laboratoire d'Etude des Materiaux pour la Microélectronique, Université de Bordeaux 1, 351 Cours de La Libération, 33405 Talence CEDEX, France

J. P. Doumerc
Laboratoire de Chimie du Solide du CNRS, 351 Cours de La Libération, 33405 Talence CEDEX, France

F. Lévy
Institut de Physique Appliquée, Ecole Polytechnique Fédérale de Lausanne, CH-1015 Lausanne, Switzerland
(Received 30 December 1991)

This paper is devoted to the study of the photoelectrochemical properties of the polyiodide solution/WSe_2 interface. Cleaved, scratched cleaved, and stepped uncleaved surfaces were used in the experiments. The photocurrent was strongly dependent on the surface conditions. Cleaved surfaces had a high photocurrent with an abnormal decrease for short wavelengths. A model based on both the results of the electrical studies given in the preceding paper and those of optical transmission measurements and atomic force microscopy is proposed and allows us to understand this behavior. Finally, the yield of the photoelectrochemical cells was measured; it was observed that the yield of stepped surfaces can be increased by oxidizing the surface.

I. INTRODUCTION

This paper mainly deals with the optical and photoelectrochemical (PEC) properties of the polyiodide electrolyte/WSe_2 interface.

In Sec. II, we report measurements of the photocurrent and optical transmission versus the wavelength below the fundamental absorption edge. Atomic force microscopy was also used to image surface defects. Cleaved, scratched cleaved, and stepped uncleaved surfaces were investigated. A simple model is proposed to describe the behavior of the photocurrent whatever the surface state may be.

In Sec. III, the conversion efficiency of the PEC cells is discussed in relation to the state of the surface. A treatment is proposed to improve the yield in case of stepped surfaces.

II. MONOCHROMATIC PHOTOCURRENTS

The photocurrent versus the wavelength was measured for various electrodes dived in the polyiodide ($2M$KI$+5\times10^{-3}M$I$_2$) aqueous electrolyte. Measurements were performed under potentiostatic conditions in a three-electrode electrochemical cell. All the spectra were recorded under a reverse potential $V_{SC/SCE}=0.3$ V, i.e., a surface potential of 0.8 V in the semiconductor,[1] where SC denotes semiconductor and SCE denotes standard calomel electrode. The electrode was illuminated through a quartz window, in the cell wall, using a 150-W tungsten iodine lamp as a light source and a monochromator (Oriel, model 7240) followed by a 590-nm cut-on filter (MTO Photovex). The light intensity was measured with a radiometer photometer (EG&G, model 550). Accurate measurements were performed by attaching a diaphragm to the head detector. The diaphragm was selected to have the same area as the electrode, i.e., 0.05 cm^2. The photocurrent was measured with a lock-in amplifier working at 20 Hz.

In Fig. 1, typical spectra corresponding to an uncleaved, cleaved, and scratched cleaved surface are shown. The highest photocurrent is obtained for a cleaved surface nearly free of defects. However, the photocurrent has an unusual behavior; it decreases for short wavelengths. Electrodes with a large amount of defects on the surface have a photocurrent which increases weakly as the wavelength decreases and reaches a plateau at short wavelengths.

Similar behaviors were obtained by various authors in

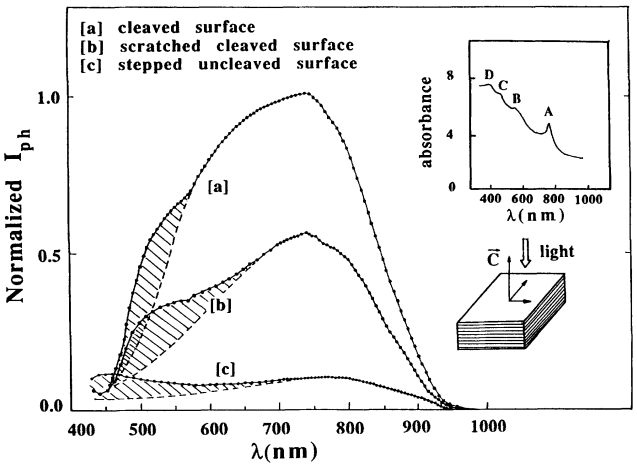

FIG. 1. Typical photocurrents vs the wavelength λ for three different states of the surface; the inset shows the absorbance vs λ. The photocurrent in the hatched zones is related to the oxidation process. Hatched zones are guides for the eyes and do not correspond to an exact calculation. Spectra have been corrected for the solution absorbance.

studying photocurrent with the same material[2–6] or other layered type semiconductors such as $MoSe_2$,[7,8] InSe,[9] . . . .

In the simple Gärtner's model, the photocurrent at a wavelength $\lambda = c\nu^{-1}$ is expressed as[10]

$$I_{\text{ph}} = \frac{q\Phi_0}{h\nu} S \left[1 - \frac{e^{-\alpha W}}{1+\alpha L_p} \right] , \tag{1}$$

where α, W, and L_P are, respectively, the absorption coefficient, the depletion width, and the diffusion length, Φ_0 is the incident power (W m^{-2}), and S the sample area. In the following we note $K_{(\nu)} = q\Phi_0/h\nu$. Recombinations inside the depletion zone are neglected in Gärtner's model. This hypothesis is well verified for a high reverse potential, i.e., a high electric field near the surface, leading to a very short transit time smaller than the carrier lifetime.

As the wavelength decreases, the absorption coefficient α increases. Most of the photons are then absorbed within a region smaller than the diffusion length L_P, and the photocurrent reaches a limit. The photocurrent of electrodes with a large amount of defects seems to follow this behavior, whereas Gärtner's law is not well suited to describe the photocurrent of cleaved electrodes. In particular it is unable to describe why the photocurrent falls down at about 750 nm. Comparing curves *a* and *b* in Fig. 1 suggests that the steps still present on cleaved surfaces are responsible for this situation.

Interference patterns of the optical transmission below the fundamental absorption show that steps are still present on large cleaved surfaces. A typical transmission spectrum of a cleaved electrode is given in Fig. 2. Beside the usual interferences due to the difference of refractive indexes between the material and the air, a modulation of the interference amplitudes is observed. Below the fundamental absorption, in the case of a weak absorption, the transmission T versus the wavelength λ is usually well described by the following formulas:[11]

$$T(\lambda) = \frac{16 n_0^2 n^2 \alpha}{1+\alpha^2-2\alpha\cos(4\pi n t/\lambda)} , \quad \alpha = \exp(-4\pi k t/\lambda) . \tag{2}$$

n and k are the real and imaginary parts of the complex refractive index of the material, respectively, t is the thickness of the sample, and n_0 is the air index.

Minima and maxima of the transmission depend on the thickness of the sample. In presence of steps the thickness is no longer a constant, thus Eq. (2) has to be modified to take into account this particular situation. From a coarse point of view, we can expect some strange behaviors when the height of the steps and the wavelength λ are of the same order of magnitude.

Assuming a rather simple model of an electrode with a single step of height h, the transmission $T(\lambda)$ can now be written as

$$T(\lambda) = \frac{S_1}{S} \frac{16 n_0^2 n^2 \alpha}{1+\alpha^2-2\alpha\cos(4\pi n t/\lambda)} + \frac{S_2}{S} \frac{16 n_0^2 n^2 \alpha}{1+\alpha^2-2\alpha\cos[4\pi n (t+h)/\lambda]} . \tag{3}$$

S is the total area of the electrode and it is divided into two areas S_1 and S_2 with $S = S_1 + S_2$. In Fig. 2, calculated spectra using Eq. (3) are plotted for four values of the height h. In our calculation, we used $k = 0.015$ and $n_0 = 3$.[12] For instance, taking $h = 500$ nm $- 1$ μm in Eq. (3) gives a relatively good fit for the experimental spectrum in Fig. 2.

Of course, the actual situation is more complicated. There is not a single step with a height h but a large step height distribution. This has been clearly observed by

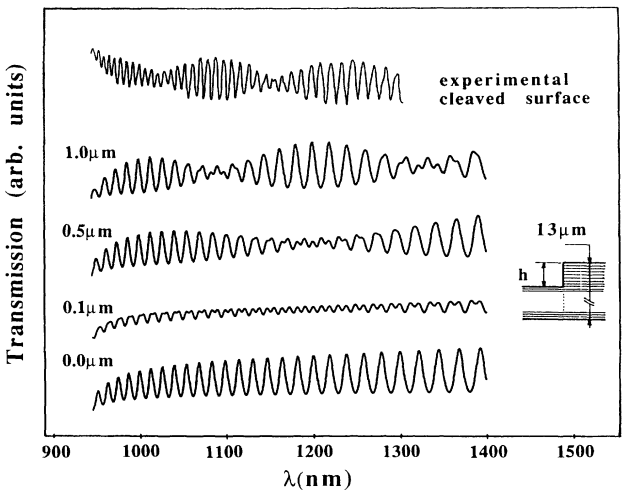

FIG. 2. Experimental and calculated transmission spectra below the fundamental absorption edge for various heights of the step.

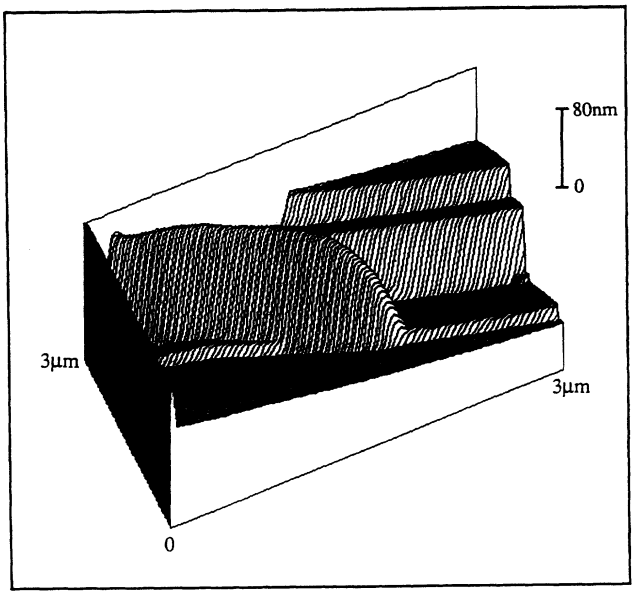

FIG. 3. Scan of a cleaved WSe_2 surface obtained by atomic force microscopy.

atomic force microscopy. Figure 3 shows a typical scan (3 μm$\times$3 μm) of a cleaved surface; steps with various heights are the sole defects encountered.

Experimentally, the influence of the steps on the shape of the photocurrent versus the wavelength is evidenced in Fig. 4. In this figure, the photocurrents measured for various wavelengths are plotted for several preparation conditions of the WSe_2 surface. The photocurrent of a freshly cleaved surface is taken as reference. We observe a decrease of the photocurrent at short wavelengths for scratched surfaces. Oxidation of the surface cancels this decrease and thus neutralizes the step effect and even enhances the photocurrent obtained for freshly cleaved surfaces.

Consequently, Gärtner's model has to be modified to take into account the effect of steps. For this purpose, we assume an electrode of area S with only one step of height h (see Fig. 5). From electrical measurements we know that equipotentials are strongly modified near a step,[1] thus the surface of the electrode is divided into three parts noted I, II, and III which have respectively S_1, S_2, and S_3 as areas. In parts I and II, the potential drop is unperturbed by the step (the electric field has its maximum close to the surface) whereas in part III the electric field is very weak as mentioned in the preceding paper. Holes which are generated in the parts I and II are normally collected at the surface and they react with I^- anions to form I_2. In these regions, the photocurrent follows Gärtner's law:

$$I_{\rm ph}=K_{(\nu)}(S_1+S_2)\left[1-\frac{e^{-\alpha W}}{1+\alpha L_p}\right] . \tag{4}$$

Because the electric field is very weak in part III, the diffusion takes place along the layers where the diffusion coefficient is higher but most of the carriers generated in this region within a depth h are recombined. Moreover, the holes reaching the surface $\parallel$ to the c axis are probably trapped by the surface defects. Consequently, carriers

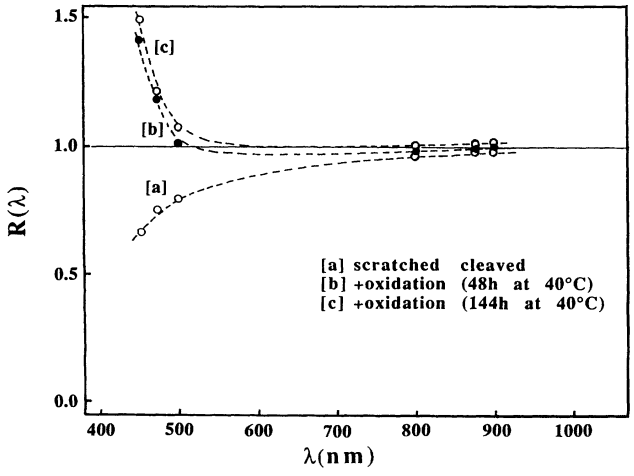

FIG. 4. Ratio for various wavelengths of the photocurrent for several treatments vs the photocurrent measured for a freshly cleaved surface.

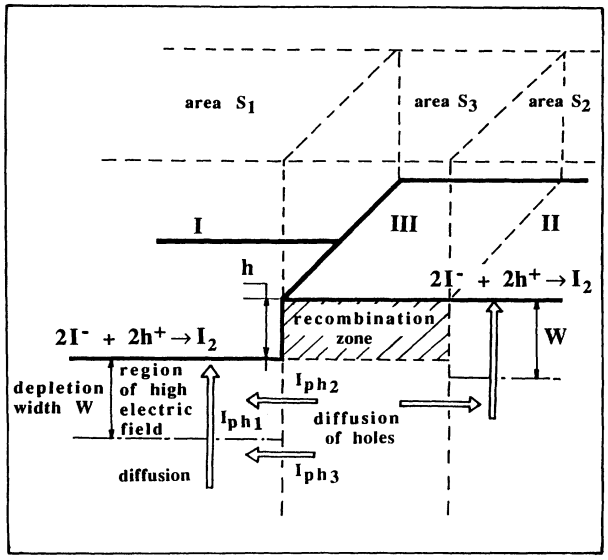

FIG. 5. Sketch of the surface near a step used in Eq. (5) to calculate the theoretical photocurrent.

generated in the volume hS_3 are lost for the photocurrent. However, the situation is different for carriers generated at a depth larger than the height h of the step. In parts I and III the hole concentrations are very weak, in particular in the depletion zone, so there is a large gradient of concentration along the layers. Due to the high value of the diffusion coefficient in the layers the holes which are generated in part III can reach parts I and II; then they contribute to the photocurrent. The total photocurrent can be coarsely written as

$$I_{\rm ph}=I_{\rm ph1}+I_{\rm ph2}+I_{\rm ph3}$$

with

$$\begin{aligned} I_{\rm ph1}&=K_{(\nu)}(S_1+S_2)\left[1-\frac{e^{-\alpha W}}{1+\alpha L_p}\right] , \\ I_{\rm ph2}&=K_{(\nu)}S_3(e^{-\alpha h}-e^{-\alpha(h+W)}) , \\ I_{\rm ph3}&=K_{(\nu)}S_3\left[e^{-\alpha(h+W)}\frac{\alpha L_p}{1+\alpha L_p}\right] . \end{aligned} \tag{5}$$

The first term $I_{\rm ph1}$ stands for the photocurrent generated in parts I and II whereas $I_{\rm ph2}$ and $I_{\rm ph3}$ are issued from part III. $I_{\rm ph2}$ is the photocurrent due to the carriers generated between the depths h and $h+W$, $I_{\rm ph3}$ for those generated below the depth $h+W$.

In Fig. 6, plots of Eq. (4) as a function of height h of the step are given for a particular value of $S_3/(S_1+S_2)=15$. These calculations use a depletion width $W=200$ nm corresponding to a reverse bias $V_{\rm SC/SCE}=0.3$ V, a diffusion length $L_p=2$ μm, and a simple square power law for the absorption coefficient $\alpha\propto(h\nu-E_g)^2/h\nu$, because the fundamental absorption is due to indirect transitions involving phonon absorption.[13,14] This was confirmed by plotting $(\eta h\nu)^{1/2}\propto(\alpha h\nu)^{1/2}$ versus the photon energy $h\nu$, as

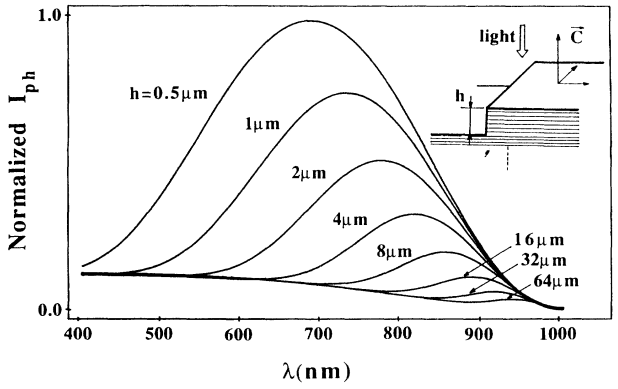

FIG. 6. Calculated photocurrents vs the wavelength λ for various heights h of the step.

shown in Fig. 7; $\eta = I_{ph}/(Sq\phi_0/h\nu)$ is the quantum yield and ϕ_0 the incident power per unit of area. An energy gap E_g of 1.27 eV was found, a value which is in good agreement with the other values encountered for this material.[14,15]

The diffusion length of minority carriers was measured for a cleaved surface by plotting $\ln[1/(1-\eta)]$ vs $(V-V_{fb})^{1/2}$ at a constant wavelength, as suggested by Eq. (1), where V_{fb} is the built-in potential. In this plot, the y-axis intercept gives $\ln(1+\alpha L_p)$, thus L_p may be obtained if the absorption coefficient α is known. A value of α is given by the slope of the plot so long as the donor concentration N_d is known; here $N_d \simeq 3.5\times10^{16}$ cm^{-3} was measured by the Hall effect and also by C-V characteristics.[1] In this manner, we obtain $L_p \simeq 2$ μm at λ=750 nm (see Fig. 8). This value is in agreement with values already measured in this material.[14,16]

However, in the presence of steps, the determination of L_p by Eq. (1) is of course a rather coarse approximation, because only a part ϕ_0' of the incident light ϕ_0 is active. As a consequence we measure an apparent value L_{pa}

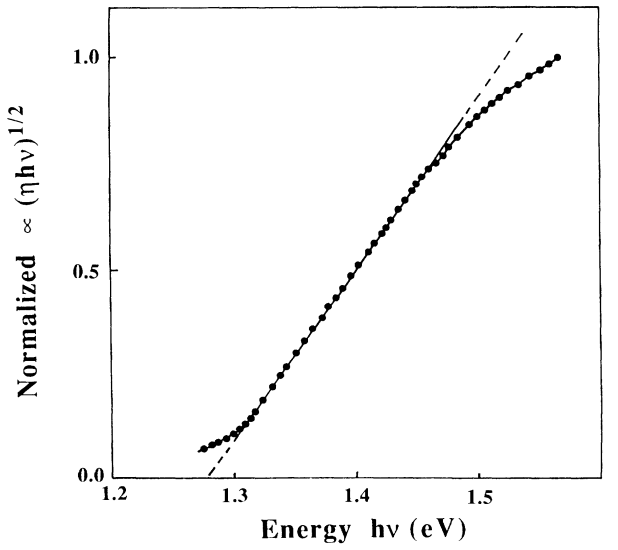

FIG. 7. Normalized quantum yield as a function of the photon energy $h\nu$, the x-axis intercept gives the absorption edge E_g.

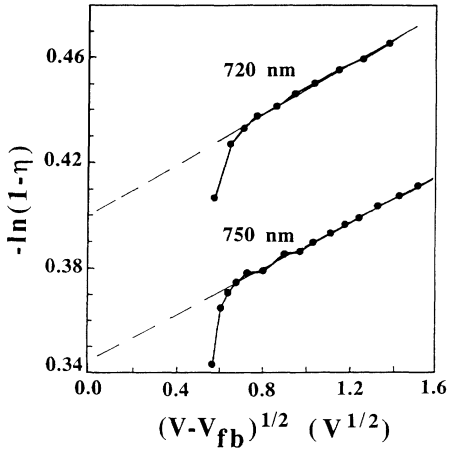

FIG. 8. Determination of the diffusion length L_p of minority carriers for two wavelengths by using the Gärtner's model.

smaller than the true value L_p. We have so far neglected the reflectivity, which is about 35% in the energy range of our concern.[17] Taking this correction into account, L_p would be 2.4 μm.

As shown in Fig. 6, Eq. (5) can describe all the experimental results, in particular the case of electrodes with a large amount of defects. For these electrodes, the surface is very stepped and the mean height h can be higher than α^{-1}, so most of the carriers generated in part III do not contribute to the photocurrent; that is the reason why the photocurrent is so weak.

Experimental photocurrents exhibit a shoulder on the short-wavelength part (see Fig. 1). This effect is not predicted by our simple model, but we know from results presented in Fig. 4 that this is related to the oxidation process. The oxidation tends to decrease the step-electrolyte conductance[1] and thus to restore a normal potential distribution near a step; consequently, the photocurrent increases.

III. PHOTOELECTROCHEMICAL EFFICIENCY

The last section of this paper is devoted to the PEC efficiency and its relation to the state of the surface.

In these experiments the electrodes were illuminated by a 150-W tungsten lamp. A water filter was set between the lamp and the three-electrode cell.

As shown in Fig. 9(a), for a cleaved electrode, the current under illumination does not depend on the reverse potential for $V_{SC/SCE} \geq 0.1$ V, it reaches $\simeq 27$ mA cm^{-2}. For large potentials, the depletion width W becomes larger than the penetration length of the light ($\simeq \alpha^{-1}$), thus in Eq. (5) the term $e^{-\alpha W} \rightarrow 1$ and the photocurrent develop a plateau. For small potentials $V_{SC/SCE}$, the electric field in the depletion region becomes smaller and the recombination through this region can no longer be neglected, thus the photocurrent decreases; this behavior is not taken into account in Gärtner's model. The photocurrent-photopotential characteristic of such an electrode is given in Fig. 9(b).

For a scratched cleaved surface the dark current is increased and the photocurrent is strongly reduced. The

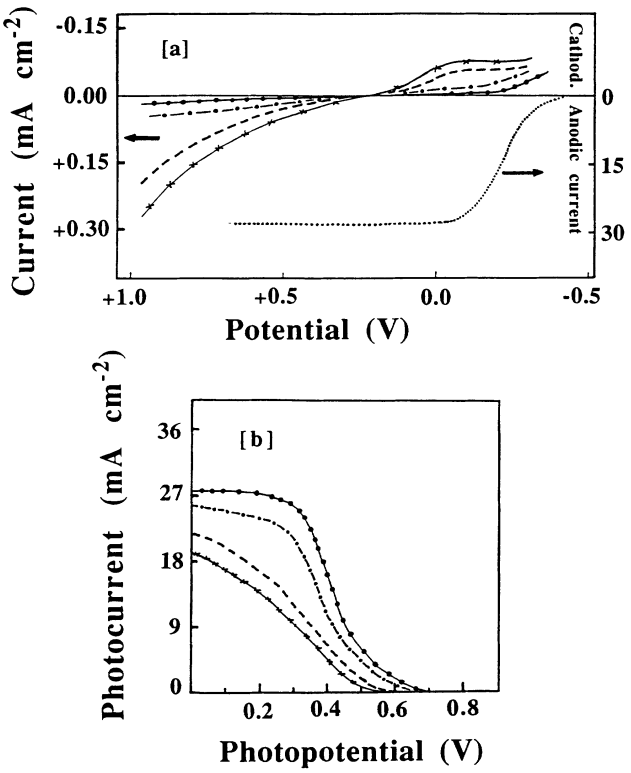

FIG. 9. (a) Dark currents and (b) photocurrent-photovoltage characteristics for a cleaved surface (•—•—•) and a scratched cleaved surface (×—×—×) followed by an oxidation at 40 °C under atmosphere during 48 h (– – –) and 90 h (–•–•–). In (a), the current under illumination for a cleaved surface is in dotted lines. The sweep rate is 1 mV s^{-1}, the potential V in (a) is referenced to the SCE.

photocurrent-photopotential characteristic of this electrode is given in Fig. 9(b). However, it is possible to improve the efficiency of these electrodes by an oxidation of the surface. We tried only oxidation at 40 °C under an atmosphere.

Results of this treatment are shown in Fig. 9(a), where the dark current versus $V_{SC/SCE}$ is plotted for various times of oxidation. The treatment has the effect of decreasing the reverse current and thus increasing the efficiency, probably by the formation of a thin oxide layer on the surface || to the **c** axis. However, the oxidation process has a limit and it is difficult to completely cancel the dark reverse current [see Fig. 9(a)].

All these results may be compared with those of the preceding paper where admittance spectroscopy measurements of electrodes || to the **c** axis have clearly shown that the electronic transfers occurring at these surfaces are considerably decreased after the oxidation process (see curve *b* in Fig. 5 of the preceding paper).

IV. CONCLUSION

The monochromatic photocurrents have been studied in relation to the state of the surface. For stepped surfaces the photocurrent is weak but it seems to follow the simple Gärtner model. The photocurrent of cleaved surfaces has an unusual behavior; it decreases at short wavelengths. Cleaved surfaces may still present steps which are clearly observed by atomic force microscopy and by optical transmission. The photocurrent begins to decrease when the inverse of the absorption coefficient is of the same order of magnitude as the height h of the step. Due to the weak value of the conductance of the step-electrolyte interface and to the WSe_2 conductivity anisotropy a large area S_3 near the step can be considered as short-circuited. The photons which are absorbed in the hS_3 volume do not contribute to the photocurrent.

Finally, we report measurements of the photoelectrochemical efficiency for various electrodes. Stepped electrodes have a weak efficiency compared to cleaved electrodes. However, we have shown that it is possible in the case of stepped surface to increase this efficiency by oxidation of the surface. The formation of a thin oxide layer on surfaces || to the **c** axis allows one to reduce the reverse dark current and thus to improve the characteristics of the device.

ACKNOWLEDGMENTS

The authors would like to thank Dr. J. P. Aimé and T. Bouhacina from LCPC-CNRS University of Bordeaux 1, for their help in atomic force microscopy.

[1]R. Bourezg, G. Couturier, J. Salardenne, and F. Lévy, preceding paper, Phys. Rev. B **46**, 15 403 (1992).
[2]H. J. Lewerenz, A. Heller, and F. J. Disalvo, J. Am. Chem. Soc. **102**, 1877 (1980).
[3]F. R. F. Fan, H. S. White, and A. J. Bard, J. Am. Chem. Soc. **102**, 5142 (1980).
[4]W. Kautek, H. Gerischer, and H. Tributsch, J. Electrochem. Soc. **127**, 2471 (1980).
[5]H. Tributsch, Ber. Bunsenges. Phys. Chem. **82**, 169 (1978).
[6]J. Gobrecht, H. Gerischer, and H. Tributsch, Ber. Bunsenges. Phys. Chem. **82**, 1331 (1978).
[7]C. Choukou-Azaiez, Thèse Université Bordeaux 1, No. 188, 1988.
[8]F. R. F. Fan and A. J. Bard, J. Electrochem. Soc. **128**, 945 (1981).
[9]C. Lévy-Clément and R. Tenne, in *Photoelectrochemistry and Photovoltaics of Layered Semiconductors,* edited by A. Aruchamy (Kluwer Academic, Dordrecht, 1992).
[10]W. W. Gärtner, Phys. Rev. **116**, 84 (1959).
[11]J. C. Manifacier, J. Gasiot, and J. P. Fillard, J. Phys. E **9**, 1002 (1976).
[12]A. Jakubowicz, D. Mahalu, M. Wolf, A. Wold, and R. Tenne, Phys. Rev. B **40**, 2992 (1989).
[13]R. Coehoorn, C. Haas, J. Dijksstra, C. J. F. Flyse, R. A. de Groot, and A. Wold, Phys. Rev. B **35**, 6195 (1987).
[14]R. Coehoorn, C. Hass, and R. A. de Groot, Phys. Rev. B **35**, 6203 (1987).
[15]R. Tenne and A. Wold, Appl. Phys. Lett. **47**, 707 (1985).
[16]D. Mahalu, A. Jakubowicz, A. Wold, and R. Tenne, Phys. Rev. B **38**, 1533 (1988).
[17]A. R. Beal, W. Y. Liang, and H. P. Hughes, J. Phys. C **9**, 2449 (1976).

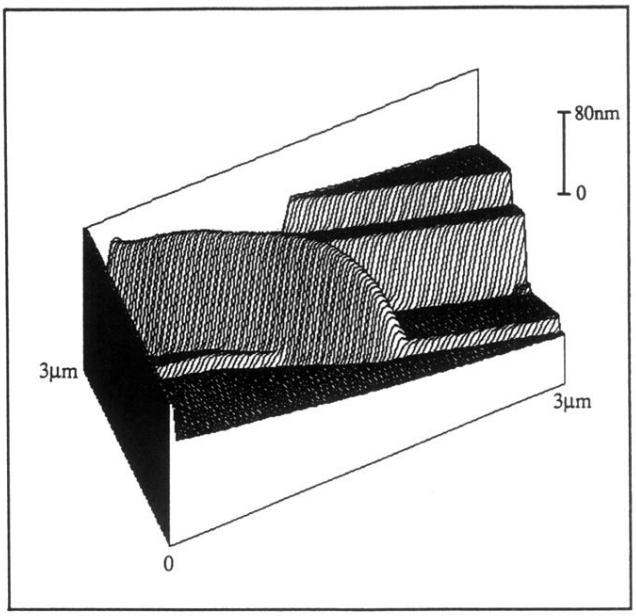

FIG. 3. Scan of a cleaved WSe_2 surface obtained by atomic force microscopy.